

Product Sequencing on a Mixed-Model Assembly Line using Deep Learning

Christoffer Lindkvist

23rd February 2026

Abstract

A Mixed-Model Assembly Line (MMAL) manufactures different product variants on a single line, where variations in tasks can cause imbalances across workstations. When several labour-intensive models appear consecutively, stations may exceed their capacity, leading to overloads that require halting the entire line. This challenge is formalized as the Product Sequencing Problem, an NP-hard optimization task traditionally managed by rule-based heuristics or human intuition.

This thesis investigates the viability of Deep Learning for solving this problem by emulating valid scheduling logic. We adapt and compare three Neural Network architectures: the **Sequence-to-Sequence (Seq2Seq)** model and the **Transformer** (originally derived from Natural Language Processing), alongside the **Pointer Network** (designed for combinatorial optimization). To overcome the limitations of inconsistent historical records, the models are trained on high-fidelity synthetic data generated via a constructive "solved puzzle" algorithm, which serves as a collision-free ground truth.

The models are evaluated on their ability to minimize station overloads in permuted sequences. Results demonstrate that the **Transformer** architecture significantly outperforms the recurrent models, achieving a **93% reduction in overloads** on unseen test data, compared to approximately 72–75% for the RNN-based approaches. These findings suggest that attention-based mechanisms are superior in capturing the global context required for complex constraint satisfaction in manufacturing.

Acknowledgements

Funding: Vinnova grant 2023-00970 (EUREKA ITEA4 ArtWork), Vinnova grant 2023-00450 (Arrowhead fPVN, Swedish funding), and KDT JU grant 2023-000450 (Arrowhead fPVN, EU funding).

Definitions

Contents

1	Introduction	5
1.1	Background	5
1.2	Research Problem	5
1.3	Objectives	6
1.4	Visualization of the Problem	6
1.5	Jump-in and Jump-out	7
1.6	Defining Drift Area	9
1.7	Defining Overlaps	10
2	State of the Art Analysis	11
2.1	Recurrent Architectures	12
2.1.1	Long Short-Term Memory (LSTM)	12
2.1.2	Sequence-to-Sequence (Seq2Seq) Models	12
2.1.3	Limitations of Recurrent Architectures	13
2.2	Attention-Based Architectures	13
2.2.1	The Transformer Model	13
2.2.2	Pointer Networks	13
3	Methodology	15
3.1	Data generation	15
3.1.1	Constants	15
3.1.2	Data Preprocessing and Abstraction	15
3.1.3	Offset Calculation and Centering	16
3.1.4	Constructive Data Generation as a Solved Puzzle	17
3.2	Adapting Language-Based Models for Sequencing	18
3.3	Workarounds	19
3.3.1	Direct Continuous Input	19
3.3.2	Soft Decoding	19
3.3.3	The Pointer Head	20

4 System Architecture	21
4.1 Machine Learning Models	21
4.1.1 The Transformer Model	21
4.1.2 Sequence-to-Sequence	23
4.1.3 The Pointer Network Model	24
4.2 The Dataset	26
4.2.1 Data Processing	26
4.2.2 Shuffled Task Generation	26
4.3 The Training Loop	27
4.3.1 Optimization and Objective Function	27
4.3.2 Regularization and Stabilization	27
4.3.3 Transformer Specifics: Masking strategy	27
4.3.4 Teacher Forcing	28
4.4 The Application Programming Interface (API)	28
4.4.1 Endpoints	28
5 Experiments and Results	30
5.1 Task Performance	30
5.1.1 Evaluation Metrics	30
5.1.2 Pointer Network Performance	31
5.1.3 Transformer Performance	31
5.1.4 Seq2Seq performance	32
5.2 Production Dataset	32
6 Discussion	33
6.1 Interpretation of Results	33
6.2 Limitations	34
6.2.1 Testing and Training Data	34
6.2.2 Hardware and Resource Limitations	34
6.2.3 Improvement Metrics	34
6.3 Future Work	34

1. Introduction

1.1 Background

This thesis addresses machine learning applied to the Product Sequencing Problem, an NP-Hard optimization problem which arises in the planning of mixed-model assembly lines [6]. A mixed-model assembly line is designed to produce various models or variants of a product on the same continuous line without setup changes between models. The core of the problem lies in the fact that different items on the assembly line may take different amounts of processing time to be completed at a given station. Thus, scheduling conflicts and work overloads may arise from two or more demanding objects being consecutively sequenced.

Traditionally, product sequences are determined manually by management staff using a rule-based framework. However, if a sequence needs to be adjusted, the process relies primarily on tacit knowledge accumulated through experience. While this often produces feasible solutions with relatively few scheduling conflicts, it remains ad hoc and sporadic. The methods used in assembly today are based on human intuition and rules that have accumulated over the years. These subtleties can prove highly restrictive in search of better solutions, and hard to teach new operators.

The main constraint for this problem is that the assembly line moves synchronously. If a single station exceeds its cycle time, then the *entire* assembly line halts. Thus, the goal of this thesis is to minimize the number of production halts.

1.2 Research Problem

Current approaches in practice often rely on human expertise and tacit knowledge, which limits scalability and consistency. If this knowledge could be systematically emulated using a model that mimics historical sequencing data, and in effect tacit knowledge, it may provide stronger starting points for any given adjustments to be made later on. Consequently, switching from a strictly rules-based to a more time-based approach could help reduce the number of overloads (1.7), and conflicts.

1.3 Objectives

The primary objectives of this thesis are:

1. **Deep Learning Framework Design:** To design a supervised learning framework capable of emulating expert scheduling logic. Due to the scarcity of consistent historical records, this involves training on high-fidelity synthetic data generated via a constructive "solved puzzle" heuristic to represent valid, collision-free ground truths, 3.1.4.
2. **Architectural Adaptation:** To adapt architectures originally designed for Natural Language Processing (Sequence-to-Sequence, Transformer) to the domain of combinatorial optimization. This includes modifying them to handle continuous feature vectors and enforcing permutation constraints via pointer mechanisms. 3.3
3. **Comparative Evaluation:** To investigate and compare the performance of Recurrent versus Attention-based architectures in resolving the Product Sequencing Problem, specifically measuring their ability to minimize station overloads, 1.7.

1.4 Visualization of the Problem

This visualization describes the flow of the assembly line along two axes: stations (S_n) and clock-cycles (T). A clock-cycle is defined as the logical step in which the assembly line advances, representing the time required for an item to move from one station to the next (referred to as **Takt**, see 3.1). In the visualization, items are stretched along the timeline to reflect their processing duration relative to this fixed window. Although the clock-cycle represents a specific unit of time in the model (700 Cmin), the visualization treats it as a relative step to illustrate sequencing logic.

Each allocation on the timeline may extend beyond its standard cycle by borrowing time from a previous or upcoming station. This borrowable buffer is referred to as the "*drift area*" (1.6). A drift area serves as a transitional zone between S_n and S_{n+1} . While both stations have permission to borrow time within this space, the physical constraint is that only one station may utilize the drift area at any single moment. This flexibility is crucial for fitting labour-intensive items onto the line without halting production. However, this shared resource is also the primary source of our scheduling conflicts.

As illustrated in Figure 1.1, item D requires additional processing time on station S_4 , $T + 2$ and is forced to utilize the drift area from both S_3 and S_5 . While this single allocation is valid, a conflict arises at $T + 2$ because the subsequent item, E , also requires the use of the shared drift area between S_4 and S_5 . Since the space cannot be occupied

by both simultaneously, this causes an overload that necessitates a line halt. Visualized as an overlap.

A similar conflict appears at T with items F and G . Both items require borrowing time from the preceding and succeeding stations. Because the available drift capacity is insufficient to accommodate the combined duration of both tasks, they create an overlap where the items *cannot* fit.

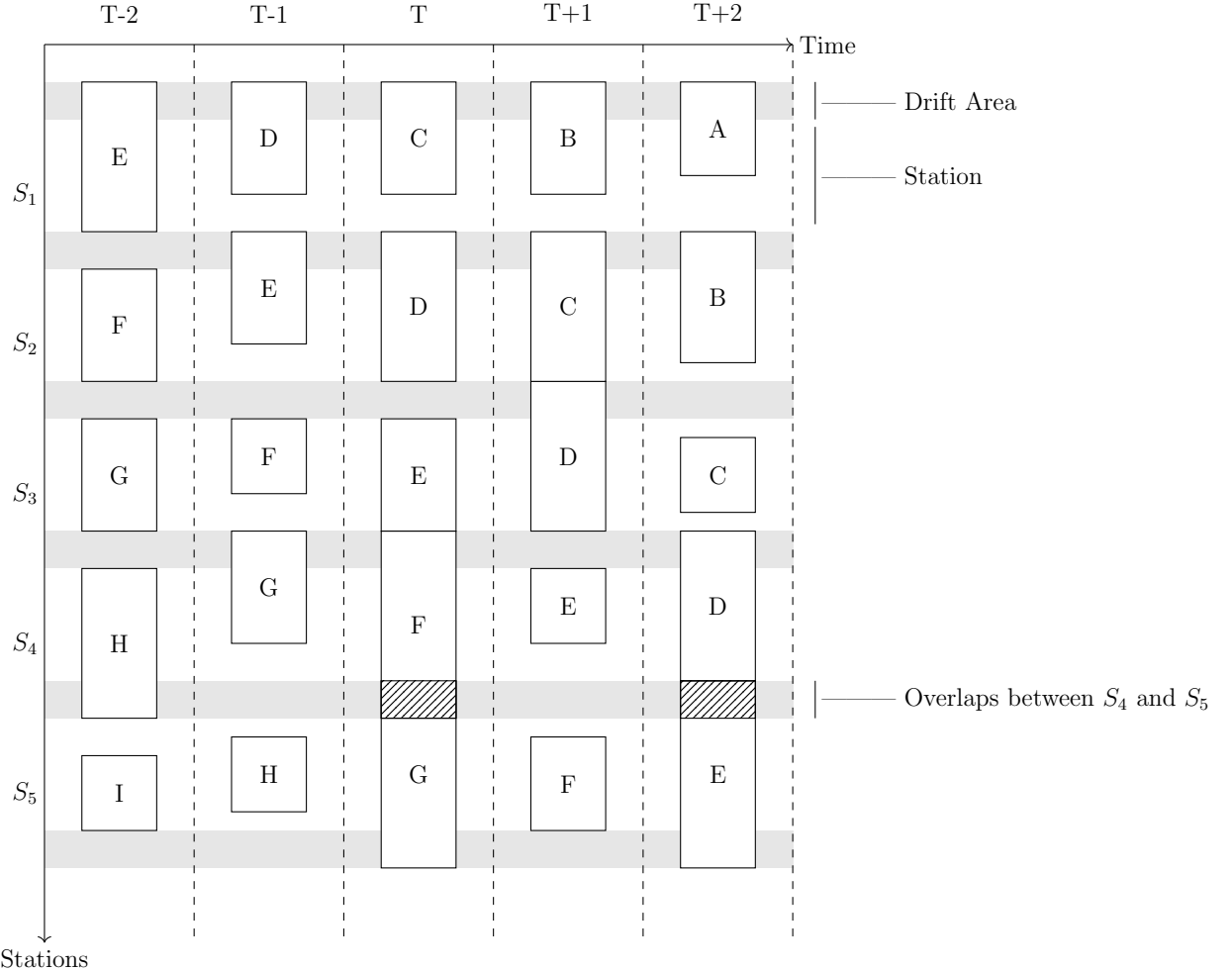


Figure 1.1: Assembly Line Example with Uniform Station and clock-cycles

1.5 Jump-in and Jump-out

In modern production, product sequences are typically finalized and staged relying on a rules-based framework, then the sequences frozen in batches before entering the assembly line. Ideally, the order will remain unchanged, but last-minute adjustments may occasionally be necessary, **this** is the part where the tacit knowledge is essential.

When a product is missing critical components and cannot be built, it shouldn't enter

the assembly line at all. In such cases, the product must be temporarily removed from the sequence and held until all parts are available, a process referred to as *jump-out*[6].

A related challenge occurs when the missing components finally arrive, since the product components occupy space on the assembly station. Ideally, jumped out product should be reintegrated into the assembly line as soon as possible, preferably before the next batch begins production. Currently, however, reintegration is delayed, and the suspended product may not re-enter the assembly line until several batches later.

The challenge in this case lies in rule-based constrictions. For example, if the sequence is built upon the rules **"1. Object A requires at least two other objects before another Object A to properly fit. 2. Object D cannot be placed next to object B."**

$$S = [A, B, B, A, C, D, D, A, C, B, A, D]$$

$$\text{Jump-in} = [A]$$

Where does *A* fit?

From an algorithmic perspective, if we disregard the rules, a *jump-in* can be treated as an $O(n \times m)$ problem: one needs only to inspect the n positions in a sequence of length n to determine the best insertion point in the upcoming batch, and then adjustments on the m remaining objects must be done. Implemented correctly, a jump-in could occur as soon as the following batch. Nevertheless, depending on operational constraints, it may not be feasible in every batch.

Jump-out, on the other hand, can be considered an $O(1)$ problem, though it presents additional practical challenges. Removing a product from the assembly line creates a gap that must be managed. This gap may require shifting a portion of the sequence by one clock cycle (T), potentially causing overloads (1.7). Alternatively, the gap could be left in place, which avoids overloading but will result in lower throughput [6].

If we return to the rule-based example,

$$[A, B, B, A, C, D, D, A, C, B, A, D] \longrightarrow [A, B, \times, A, C, D, D, A, C, B, A, D]$$

$$\text{Jump-out} = [B]$$

In the worst case several products may need to be resequenced in order for a solution to be found, rather than a single insertion.

1.6 Defining Drift Area

The Drift Area is visualized in this thesis as a gray zone intersecting two neighbouring stations, it is also the source of our scheduling conflicts. The Drift Area allows for a lot of flexibility due to the fact that *instead* of slowing down the assembly line to 1100 Cmin and decreasing the production output by roughly 40%, the assembly line instead moves at a pace of 700 Cmin per station 3.1, with 200 Cmin available as *drift* on both sides.

For a station S_n (where $Takt = 700$ Cmin), we can use up to 200 Cmin from S_{n-1} and up to 200 Cmin from S_{n+1} . This is referred to in this thesis as **Borrowing**. Borrowing this way will give us up to a total time of 1100 Cmin for any given task T_n , with the caveat of S_{n-1} and S_{n+1} being reduced to a minimum of 500 Cmin.

It is also important to note that while an object T_n is borrowing from S_{n+1} , work cannot begin on the subsequent object T_{n+1} until the borrowing has finished. Furthermore, while the drift area between two stations is often illustrated as two conjoined zones, the drift area of a specific station (D_{S_n}) should always be considered an extension of S_n , even though it may physically overlap with S_{n+1} or S_{n-1} .

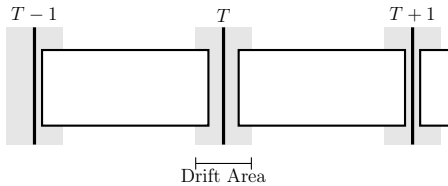


Figure 1.2: Two objects whose $Size_{T_n} < Takt$. This is the most common case, as opposed to the more extreme cases shown in this thesis.

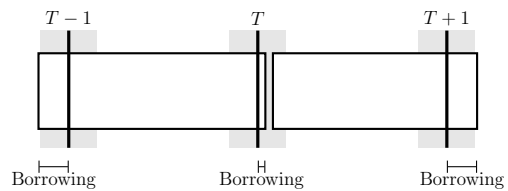


Figure 1.3: Two objects whose $Size_{T_n} > Takt$. Both need to borrow time from their neighbouring stations in order to finish in time.

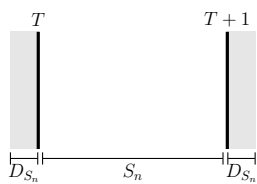


Figure 1.4: A station on its own can be depicted with one drift area at the start, and at the end of its allocated time.

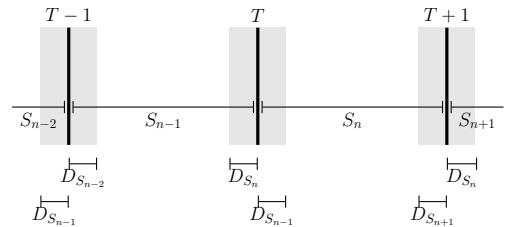


Figure 1.5: While the stations are concatenated, the drift areas will be displayed as one unit, but S_n will borrow *only* if it uses D_{S_n} .

1.7 Defining Overlaps

Overlaps stem from timing dependencies: each item's "size" on a station S_n depends on how long it takes for the item to process at the station. In other words, the "size" of the task is the duration of the task relative the duration of the station. If a task exceeds **Takt** in duration, then the use of the drift area is mandatory.

However, if two items are processed consecutively at station S_n , and both of those items exceed **Takt** in S_n to the point of requiring the usage of both of its neighbouring stations (S_{n-1} and S_{n+1}), then there *will* not be sufficient time for all operations to complete if both of those objects need to borrow time. These conflicting dependencies result in what's visualized as (and defined in this thesis as) an overlap, there simply isn't enough time for assembly to finish in time.

In practice the items do not literally stack or collide. Rather, the assembly line must halt in order to allow the operation to complete before the assembly line may continue again.

Overlaps are how station overloads are visualized in this thesis, as we follow the constraint that no matter what, an allocation can never exceed $Takt + 2 * Drift$ in size, and an allocation can never go past the right-most limit of the drift area on the coming station.

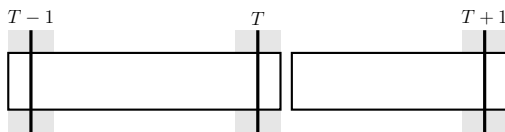


Figure 1.6: An example of two allocations, where there is enough room to borrow time for the larger one.

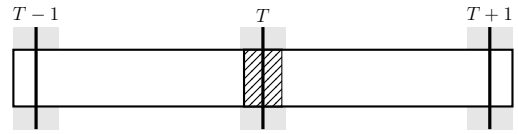


Figure 1.7: An example of two allocations, where there is not enough room as both require borrowing, causing an overload.

2. State of the Art Analysis

The Mixed-Model Assembly Line (MMAL) problem is an optimization problem, formally classified as NP-Hard[6]. Traditionally, these optimization problems are addressed using heuristic or meta-heuristic algorithms, rather than using machine learning [3].

In recent years, Deep Reinforcement Learning (DRL) has become a dominant approach for solving dynamic scheduling problems. Unlike supervised methods, DRL agents learn through trial-and-error interaction with a simulation environment, aiming to maximize a cumulative reward signal [19, 20].

For example, Chen et al. proposed an Adaptive Deep Q-Network, which builds on the Q-Learning Algorithm in order to address scheduling in Cloud Manufacturing environments characterized by stochastic task arrivals. Their approach utilizes a resizable network structure to adapt to changing machine availability and employs a complex reward mechanism to balance multiple objectives, such as minimizing work time, and optimizing machine load [10].

A primary constraint of this research is the restriction to synthetic data, without access to a live production environment or a verified feedback loop. Reinforcement Learning (RL) relies on the ability to execute actions and receive immediate rewards. Without an interactive environment or a validated simulator to provide this feedback, training an RL agent is infeasible. Therefore, this study approaches the problem through Supervised Learning. This paradigm leverages the available "solved" instances to train a model to mimic expert sequencing patterns, circumventing the need for the interactive state-space exploration required by RL agents.

Furthermore, while DRL is effective for dynamic environments where rules change frequently, it introduces complexity that goes beyond simple resource constraints. Even if a simulator were available, the careful engineering of state and action spaces remains a significant hurdle. Additionally, the "black box" nature of the reward signal makes it difficult to capture the nuanced, unwritten knowledge of the human servicemen, which is the primary objective of this thesis.

Current manual approaches rely heavily on knowledge accumulated through experience that is difficult to articulate as explicit rules, especially if rules have accumulated over time. This thesis proposes capturing this knowledge using Supervised Learning, a paradigm formally known in this context as Imitation Learning [11].

A precedent for this methodology is established by Dupuis et al. [2], who successfully trained a Sequence-to-Sequence (Seq2Seq) model using teacher-forcing to generate production schedules. More recently, however, attention-based architectures have shown promise in this domain. Youssef et al. [14] applied Transformers to autonomous task scheduling, while Giannoulis et al. [13] demonstrated their efficacy in solving combinatorial problems through trial and error.

2.1 Recurrent Architectures

To emulate the sequential decision-making process of human schedulers, we first investigate architectures adapted from Natural Language Processing (NLP) that process data sequentially.

2.1.1 Long Short-Term Memory (LSTM)

In previous works addressing similar scheduling problems, researchers have applied Recurrent Neural Networks (RNNs), often utilizing Long Short-Term Memory (LSTM) units within a sequence-to-sequence (Seq2Seq) framework [2].

A defining characteristic of LSTMs is their ability to selectively forget irrelevant information via the "forget gate." This mechanism helps the model focus on relevant patterns over time, which fixes the vanishing gradient problem found in standard RNNs [4, 9, 17]. Furthermore, LSTMs have shown they can handle difficult multi-step forecasting tasks, suggesting they are stable enough for scheduling applications [21].

2.1.2 Sequence-to-Sequence (Seq2Seq) Models

Seq2Seq models are typically built upon encoder-decoder RNN architectures. They are designed to map an input sequence to an output sequence of a different length or order [2]. While traditionally used for machine translation (e.g., transforming English to Swedish) [16], this architecture is adaptable to the assembly line problem. In this context, the input is a set of product orders, and the output is the sorted production sequence [3].

However, applying standard Seq2Seq models to permutation problems presents a specific challenge: **the fixed vocabulary**. Standard NLP models select outputs from a fixed "dictionary" of words. In a manufacturing context, every day's product list is unique. Therefore, a fixed dictionary is insufficient. The model must instead learn to select from the dynamic input available that day, treating the input as a set rather than a fixed sequence. This is difficult for standard Seq2Seq architectures unless they rely on abstract indices [2, 3, 18].

2.1.3 Limitations of Recurrent Architectures

Despite their historical success, RNN and LSTM-based models suffer from a significant bottleneck: **sequential processing**. Because these models must process the input step-by-step (item t depends on item $t - 1$), they cannot run in parallel. This results in slower training times and, more importantly, a limited ability to capture the global context of the entire schedule at once [4].

This limitation motivates the shift toward **Attention-based approaches**, which process the entire sequence simultaneously. The concept of attention was initially introduced to align inputs and outputs in RNNs [16], but later evolved into standalone architectures.

2.2 Attention-Based Architectures

2.2.1 The Transformer Model

To address the sequential bottlenecks of RNNs, Transformer-based architectures remove recurrence entirely, relying instead on a self-attention mechanism [5]. This architecture often uses Layer Normalization to stabilize training [1].

The defining characteristic of the Transformer is the use of scaled dot-product attention, also known as Multi-Head Attention. This allows the model to weigh the importance of each element in a sequence relative to all other elements, regardless of distance [14]. This parallel computation not only speeds up training but enables the model to capture global dependencies more effectively than RNN-based methods. Since Transformers do not inherently know the order of input, positional encodings are added to the input vectors to retain sequence information [5, 12].

For combinatorial scheduling problems, this means the model can see complex interactions across the entire day’s plan [13]. The placement of one item can be directly influenced by all others in the sequence, providing the context awareness necessary for effective scheduling [8].

2.2.2 Pointer Networks

While Transformers excel at context, they still typically rely on predicting tokens from a fixed vocabulary. The **Pointer Network** is the architecture in this analysis most specifically designed for combinatorial optimization [7].

Implemented using an encoder-decoder structure, the Pointer Network utilizes a specialized attention mechanism. Instead of predicting a value from a dictionary, it generates context vectors that “point” to specific elements in the input sequence.

This model is explicitly designed for problems where the output is a rearrangement of the input, such as the Traveling Salesman Problem [7, 13]. It is thus well-suited for

the Mixed-Model Assembly Line (MMAL) problem, as the object attributes (such as station order or station time) cannot be changed, thus the only goal is to find the best permutation.

3. Methodology

3.1 Data generation

3.1.1 Constants

For data generation the following constants are used:

Table 3.1: Table of Constants used in Data Generation

Constant	Default Value	Description
Objects	100	Total number of objects in the testing sequence.
Stations	39	Total number of stations.
Takt	700	The duration of a station ($Cmin$).
Drift	200	The duration of one drift area for S ($Cmin$)
Gap	10	Minimum amount of time ($Cmin$) between generated objects.
min_size	100	Shortest possible duration of an object ($Cmin$).
max_size	$Takt + 2 \times Drift$	Largest possible duration of an object ($Cmin$).
Multiplier	5000	Constant value to multiply <i>Objects</i> with, used for Training.

3.1.2 Data Preprocessing and Abstraction

For the purpose of training optimization, the raw information is abstracted into a concise JSON schema. Each entry in the dataset is reduced to the following three attributes:

- **Object ID (object)**: An integer representing the unique identifier of the item.
- **Station Data (data)**: A mapping of station keys (s_1, \dots, s_{35}) to their respective time requirement values.
- **Station Offsets (offsets)**: A mapping of station keys to their relative offset values.

By utilizing these values, we can train a model to prioritize time-based decision-making over rigid rule-based systems. It is important to note that while the model operates without explicit constraints, the use of a sufficiently large dataset derived from

expert tacit knowledge ensures that it implicitly adheres to fundamental ground rules, albeit with greater flexibility.

3.1.3 Offset Calculation and Centering

The positioning of an object within a station is determined by its *offset* relative to the **Takt** start (0 locally). The script employs a dynamic centering logic that positions tasks within the remaining available capacity of the standard Takt window. This approach balances the empty space on either side of the allocation, adapting to the finish time of the preceding task.

To determine the position, the script first calculates the local start time, t_{start} , which corresponds to the completion of the previous allocation relative to the current Takt. The remaining time B , is calculated as the difference between the standard Takt duration T and the occupied time, clamped to zero to ensure non-negative spacing:

$$B = \max(0, T - t_{start} - S) \quad (3.1)$$

Where S is the size (duration) of the new task. The tentative offset, O_{calc} , is then derived by placing the task at the start position plus half of the calculated buffer:

$$O_{calc} = t_{start} + \frac{B}{2} \quad (3.2)$$

This formula ensures that if the previous task finishes early, the new task is centered in the empty space. However, if the previous task finishes late, the buffer shrinks, effectively pulling the new task closer to the previous one.

Finally, to ensure the object adheres to physical station boundaries and drift limitations (D), the calculated offset is clamped. The maximum permissible offset is defined such that the task end does not exceed the drift area ($T + D$):

$$O_{calc} = \max(-D, \min(O_{calc}, T + D - S)) \quad (3.3)$$

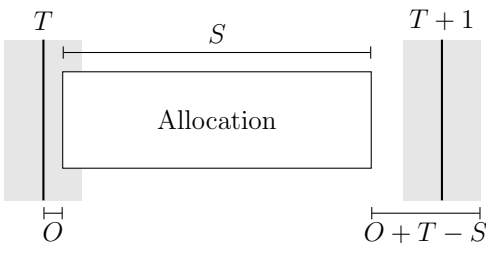


Figure 3.1: Allocation positioning before the centering process

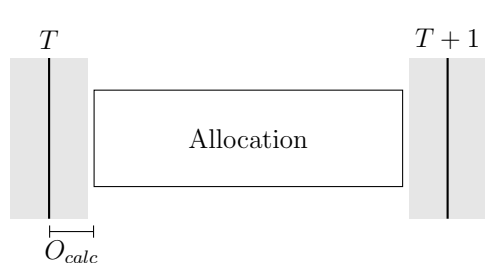


Figure 3.2: Allocation after centering.

3.1.4 Constructive Data Generation as a Solved Puzzle

To train the machine learning model, a synthetic dataset is required that represents valid, collision-free production schedules. Rather than placing tasks stochastically and checking for validity, the system employs a constructive generation algorithm which builds one object at a time. This approach acts as a forward simulation, placing allocations sequentially to inherently create a "solved puzzle" which serves as the ground truth for training. Because the entire sequence generates left to right the risk for overlaps is nonexistent.

Dependency-Based Positioning

The placement of any given allocation $A_{[T_n, S_n]}$ (Timeslot T_n at Station S_n) is not independent. It is strictly constrained by two boundaries derived from the existing grid state:

1. **Station Availability:** The station S_n must be free. Therefore, $A_{[T_n, S_n]}$ cannot start until the previous object at T_{n-1} has departed station S_n .
2. **Object Availability:** The object at T_n must be ready. Therefore, $A_{[T_n, S_n]}$ cannot start until the object at T_n has finished processing at the previous station S_{n-1} .
3. **Gap (Density control):** To vary the complexity of the generated data, a gap is introduced (3.1). A larger gap will result in sparser schedules with multiple valid solutions, whereas a minimal gap will result in densely packed schedules. In a real-world manufacturing context, tighter schedules would maximize throughput but place higher strain on human operators.

Mathematically, the earliest valid start time (t_{start}) for the new allocation is defined as the maximum of these two completion timestamps, plus a configured safety gap:

$$t_{start} = \max(End_{T_{n-1}, S_n}, End_{T, S_{n-1}}) + Gap \quad (3.4)$$

This logic ensures that the generated schedule is causally valid, no object effectively "teleports" between stations, and no two objects overlap on a single station.

Context-Aware Scaling

The dimensions of the tasks are also generated dependently. While duration in each station for each object is chosen stochastically, the actual assigned size (S) of the duration is clamped by the remaining available time in the Takt + Drift window. The generator calculates the available space between the calculated t_{start} and the maximum drift

boundary. If the size exceeds this space, it is truncated to fit (within the constraints of *min_size*, 3.1)

$$\text{min_size} \leq S \leq \text{max_size} \quad (3.5)$$

When training, the model is fed the sorted list, the solved puzzle, then while testing the model, it is fed never seen before data which has been shuffled beforehand. This process results in a synthetic dataset where every input sequence has a perfectly matching output sequence that is guaranteed to be solvable, providing a robust target for supervised learning.

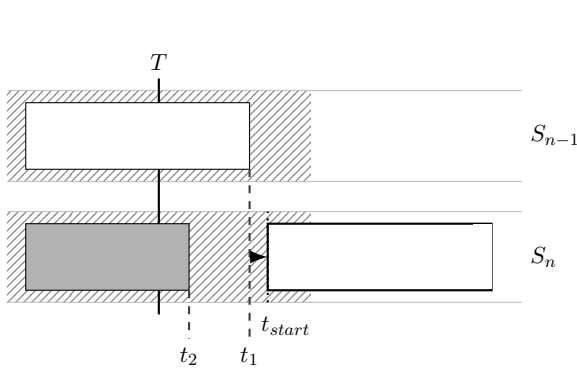


Figure 3.3: Case 1: The white object in S_{n-1} is borrowing time from itself at S_n , and thus cannot begin assembly at S_n until it has finished the task at S_{n-1} .

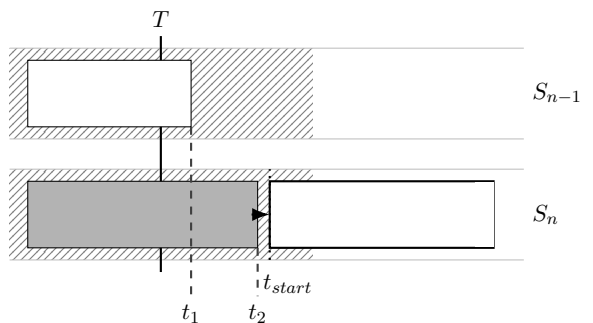


Figure 3.4: Case 2: The gray object is borrowing time from the white object in S_n . Even though it finished in S_{n-1} , the white object cannot begin assembly right away in S_n as it's dependent on the gray object finishing at S_{n-1} .

3.2 Adapting Language-Based Models for Sequencing

Two of the models examined in this thesis, the Sequence-To-Sequence model and the Transformer model, were originally designed for natural language processing (NLP) tasks. These models typically rely on a fixed, predefined vocabulary.

This reliance proves problematic because the processed data in this thesis does not consist of static words from a dictionary, rather a dynamic set of *unique* objects that changes with every production batch. Consequently, the model cannot predict a token from a learned list, rather it must instead select from the variable input provided on that sequence.

Furthermore, specific combinatorial constraints must be imposed. Natural language

generation is probabilistic and inherently allows for repetition, and if poorly trained might default to the "easiest" alternative. (e.g., the word "the" repeating multiple times, due to it being the most common word in the English language).

In our use-case, each object within the input *must* appear in the output sequence *exactly once*, and the length of the output sequence *must* match the length of the input sequence. Therefore, the architecture must be adapted to enforce this combinatorial constraint, ensuring valid permutations rather than simply generating the most statistically probable tokens (3.3).

3.3 Workarounds

The Transformer and Sequence-To-Sequence models have been adapted from their original NLP architectures to a permutation architecture in order to address combinatorial problems. The Pointer Network remains unaffected by these modifications.

3.3.1 Direct Continuous Input

The Sequence-To-Sequence model is implemented here without an Embedding layer. Instead of projecting vocabulary indices into a latent embedding space, this module is omitted to allow raw feature vectors to be processed directly. This enables the model to interpret the specific magnitudes and geometric properties of input elements as continuous values rather than abstract symbols. This approach is particularly well-suited for combinatorial tasks, as it preserves intrinsic numerical relationships in the data that would otherwise be obscured by tokenization.

3.3.2 Soft Decoding

The Sequence-To-Sequence model employs a "soft" feedback loop during sequence generation. In traditional language processing, the decoder typically commits to a single discrete choice by selecting the most probable word and treating it as the ground truth for the subsequent step. In this context, however, rigid early choices can trap the model in sub-optimal paths. To mitigate this, the model feeds the full probability distribution into the next step rather than a single discrete selection. By propagating uncertainty rather than discarding it, the system can dynamically refine its strategy as the output sequence is constructed. This works in tandem with the teacher forcing training method. (See 4.3)

3.3.3 The Pointer Head

The greatest deviation from the canonical Transformer is the removal of the vocabulary projection layer. It is replaced by a **PointerHead** module designed to select elements from the input sequence, a mechanism inspired by the Pointer Network 4.1.3.

Instead of predicting a token from a fixed vocabulary, the Pointer Head computes a similarity score between the current decoder state and the encoder outputs using the Transformer’s attention mechanism, rather than additive attention [5] [7]:

$$\text{Scores} = \frac{(Dec_{out}W_q) \cdot (Enc_{out}W_k)^T}{\sqrt{d_{model}}} \quad (3.6)$$

These raw logit scores represent the compatibility between the current decoding step and every element in the input sequence. When passed through a Cross-Entropy loss function during training, they effectively train the model to ”point” to the correct input index for the next position in the sequence.

4. System Architecture

4.1 Machine Learning Models

The models in this thesis are implemented using PyTorch.

Table 4.1: Hyperparameters and Model Constants

Constant	Transformer	Sequence-To-Sequence	Pointer Network
batch_size	16	16	8
num_epochs	10	10	10
lr	$1e^{-3}$	$1e^{-4}$	$1e^{-4}$
d_model	256	256	256
dropout	0.1	0.2	
hidden_dim		128	128
d_ff	512		
n_heads	8		
n_layers	3		

4.1.1 The Transformer Model

The implemented model adapts the standard Transformer architecture originally proposed by Vaswani et al. [5] to handle continuous combinatorial data. Unlike standard NLP models that process discrete tokens, this implementation operates on continuous feature vectors and utilizes a pointer mechanism for output generation.

Continuous Input Embeddings

Standard Transformers typically utilize a lookup table to map discrete vocabulary indices to dense vectors. Since the input data for this problem consists of continuous immutable features (station order, station times, dimensions), the embedding layer is replaced by a learnable linear projection.

Positional Encoding

As the Transformer architecture contains no recurrence or convolution, it can thus not distinguish the order of the input objects, essentially treating it as an unordered set. To address this, a fixed sinusoidal Positional Encoding is added to the input embeddings. This provides each element with a unique geometric signature, allowing the model to determine the relative positions of objects within the sequence. The encodings are calculated as [5]:

$$PE_{(pos,2i)} = \sin(pos/10000^{2i/d_{model}}) \quad (4.1)$$

$$PE_{(pos,2i+1)} = \cos(pos/10000^{2i/d_{model}}) \quad (4.2)$$

This mechanism allows the model to distinguish between identical tasks placed at different positions in the sequence.

Layer Normalization and Pre-Norm Formulation

The system employs Layer Normalization to stabilize training [1], specifically adopting "Pre-Normalization" where the input is normalized *before* passing it to the sub-layer, rather than after. This configuration, implemented in the `ResidualConnection` module, allows gradients to flow more directly through the network, generally improving convergence in deeper models.

Multi-Head Attention

The core mechanism of the model is Multi-Head Attention (MHA), which allows the model to jointly attend to information from different representation subspaces. The implementation utilizes h parallel heads. For each head, the input is projected into Query, Key, and Value (Q , K , V) matrices. The attention scores are computed using Scaled Dot-Product Attention [5]:

$$\text{Attention}(Q, K, V) = \text{softmax} \left(\frac{QK^T}{\sqrt{d_k}} \right) V \quad (4.3)$$

Feed-Forward Block

Each encoder and decoder layer contains a position-wise Feed-Forward Network (FFN). This consists of two linear transformations with a ReLU activation function in between [5]:

$$FFN(x) = \text{ReLU}(xW_1 + b_1)W_2 + b_2 \quad (4.4)$$

The inner layer projects the input to a higher dimension (d_{ff} , typically $4 \times d_{model}$) before projecting it back, introducing additional non-linearity to the model.

The Pointer Head

This implementation of the Transformer replaces the vocabulary projection layers in favour of a Pointer Head in order to handle combinatorial tasks rather than NLP-based tasks. 3.3.3

4.1.2 Sequence-to-Sequence

The implemented model is a standard Sequence-To-Sequence model with modifications clarified in 3.3.

Continuous Input Encoder

The `EncoderRNN` processes the input sequence to generate a latent representation of the problem state. Unlike standard NLP encoders that require an embedding layer to project discrete tokens, this module accepts raw feature vectors directly [4, 8].

Attention Mechanism

To overcome the bottleneck of compressing the entire sequence into a single fixed-length vector, the model employs an Attention mechanism, referred to as Bahdanau Attention [16]. This approach allows the decoder to "search" the entire input sequence and dynamically focus only on the information relevant to the current step.

Rather than relying on a static summary of the input, the mechanism calculates a dynamic "relevance score" for every item in the input sequence. These scores effectively function as a spotlight, determining how much focus the model should place on each specific input element when generating the next part of the output.

These scores are normalized into probabilities that sum to 100%. Finally, the model computes a time dependent Context Vector (c_t), which is a weighted average of the inputs [16]:

$$c_t = \sum_{j=1}^{T_x} \alpha_{tj} h_j \quad (4.5)$$

This weighted sum ensures that the model prioritizes the most relevant information for the immediate prediction while ignoring irrelevant noise, effectively bypassing the long-term memory limitations of standard Recurrent Neural Networks.

Context-Aware Decoder

The decoder (`DecoderRNN`) generates the output sequence step-by-step. To maximize the utility of the attention mechanism, the context vector c_t is injected at two distinct points in the decoding step:

- 1. Input Feeding:** The context vector is concatenated with the input of the current time step before being passed to the LSTM.
- 2. Output Projection:** The context vector is concatenated with the LSTM output before the final linear projection layer.

This structure ensures that both the recurrent processing and the final prediction are directly conditioned on the relevant parts of the source input.

4.1.3 The Pointer Network Model

The proposed solution implements a Pointer Network architecture adapted from Vinyals et al. (2015) [7]. The model follows an Encoder/Decoder paradigm enhanced with an attention mechanism, specifically designed to handle variable-length input sequences and output a permutation of the input indices.

Encoder Mechanism

The encoder processes the input sequence to generate a latent representation of the problem state.

- 1. Input Projection:** Raw input features are first passed through a **Projector** block. This module consists of a Linear Transformation, an Tanh Activation, and Layer Normalization [1].
- 2. Bidirectional LSTM:** The projected features are fed into a bidirectional LSTM. This allows the model to capture context from both past and future states in the sequence.

Decoder and Attention Mechanism

The decoder generates the output permutation one index at a time. Unlike standard NLP models that generate new tokens from a fixed vocabulary, this decoder selects indices directly from the input sequence.

- **Glimpse Mechanism:** To enhance the pointing accuracy, the model employs a "glimpse" mechanism as proposed by Vinyals et al. (2016) [18]. Unlike the standard Pointer Network which points immediately, this mechanism allows the decoder to "reason" about the global context before making a selection. At time step t , the decoder state s_t queries the encoder outputs to calculate a context vector c_t [18]:

$$c_t = \sum_{i=1}^T \text{Attention}(s_t, h_i) \cdot h_i \quad (4.6)$$

This vector summarizes the most relevant parts of the input sequence for the current decision.

- **Pointer Selection:** The final selection is performed by fusing the glimpse context with the original state. The context vector c_t is projected and added to the current decoder state (a residual connection) to form a *refined query* u_t :

$$u_t = s_t + \tanh(W_{proj} \cdot c_t) \quad (4.7)$$

This refined query u_t is then used to compute the final attention scores (logits) over the input elements. The index with the highest probability is selected as the next element in the permutation.

Masking and Inference

To ensure the validity of the resulting permutation (i.e., the Traveling Salesman constraint that every city is visited exactly once), a masking mechanism is applied during inference.

Once an input index k is selected, it is masked out by setting its log-probability to $-\infty$ ($1e^{-9}$) for all subsequent steps. This hard constraint prevents the model from selecting the same element twice. Furthermore, the model is auto-regressive: the feature vector of the selected element h_k is used as the input to the decoder for the next time step $t + 1$.

4.2 The Dataset

To train the models, a custom PyTorch Dataset was implemented to handle combinatorial data. This pipeline is responsible for converting raw input jsons into tensors. The dataset structure is identical for all models.

4.2.1 Data Processing

The dataset is initialized with raw JSON files containing sequences of station data. The pipeline flattens these structures into a $M \times N$ stack of tensors, where each tensor represents a single task sequence with the shape:

$$X = \begin{bmatrix} x_{1,1} & x_{1,2} & \dots & x_{1,N} \\ x_{2,1} & x_{2,2} & \dots & x_{2,N} \\ \vdots & \vdots & \ddots & \vdots \\ x_{M,1} & x_{M,2} & \dots & x_{M,N} \end{bmatrix} \quad (4.8)$$

Where M is the the number of objects and N is the number of stations.

The feature extraction is performed by selecting specific keys ($s_1 \dots s_N$) from the raw data objects. To ensure numerical stability and faster converges the data is then normalized using:

$$x_{norm} = \frac{x_{raw}}{1000.0} \quad (4.9)$$

Due to memory constraints, the sequences exceeding the maximum defined length are chunked into smaller subsequences to manage memory constraints effectively. (6.2.2)

4.2.2 Shuffled Task Generation

The dataset stores the ground truth sequences in their correct, sorted order. However, the data is effectively augmented during the training phase by randomly shuffling the input sequence at every iteration. This stochastic approach ensures that the model *never* encounters the same sequence twice.

To accommodate this shuffling, the target vector is dynamically generated to represent the specific indices required to reconstruct the original order from the disordered input. If the shuffled input is denoted as X' and the original sorted sequence as X , the target index y_t for time step t is calculated to satisfy the condition:

$$X'[y_t] = X_t \quad (4.10)$$

This formulation specifically trains the Pointer Mechanism of the Transformer and Pointer Network to identify the location of the next correct element within the provided input

set. (And then ”point” to it)

4.3 The Training Loop

To ensure a fair and consistent evaluation, a standardized training pipeline is implemented across all three architectures (Seq2Seq, Pointer Network, and Transformer). The training logic is built using the PyTorch framework and orchestrates data loading, gradient optimization, and model persistence.

4.3.1 Optimization and Objective Function

Model parameters are optimized using the **AdamW** algorithm [15]. This optimizer was selected for its ability to decouple weight decay from adaptive gradient updates, a modification that consistently yields better generalization than the standard Adam implementation. The learning rate is set to 1×10^{-4} and the weight decay is set to 1×10^{-2} .

The model is trained to minimize the **Cross-Entropy Loss** between the output logits and the target sequence. A masking constraint (`ignore_index=-1`) is applied to handle variable sequence lengths within batches. This effectively isolates the padding tokens from the objective function, ensuring the optimization focuses solely on valid data elements rather than padding.

4.3.2 Regularization and Stabilization

Training deep neural networks, particularly those involving recurrence (RNNs), can be unstable due to the exploding gradient problem [17]. To mitigate this, Gradient Clipping is applied to the model parameters. This acts as a safety mechanism that caps the maximum possible step size during backpropagation. By preventing drastic weight updates, it ensures that outliers in the training data or instabilities in the recurrent layers do not cause the optimization process to diverge.

4.3.3 Transformer Specifics: Masking strategy

Unlike the recurrent models, which process data sequentially by definition, the Transformer processes the entire sequence in parallel. To replicate the sequential nature of the problem and prevent information leakage, a dual-masking strategy is implemented within the training loop via the `make_masks` function:

1. **Padding Mask (Source):** This mask identifies padding tokens in the input batch. It forces the self-attention mechanism to assign zero attention weights to these positions, ensuring the model focuses only on valid tasks.

2. **Look-Ahead Mask (Target):** To preserve the auto-regressive property, a triangular "no-peek" mask is applied to the decoder. This ensures that when generating the prediction for position t , the model can only attend to positions 0 through $t - 1$, effectively hiding future ground-truth tokens.

4.3.4 Teacher Forcing

The method of training used in this thesis is referred to as "Teacher Forcing". The model is trained by supplying the ground-truth tokens from the previous time step ($t - 1$) as input to predict the current time step (t), rather than feeding back the model's own generated prediction. This stabilizes training and enables faster convergence, especially in RNN-based models [2, 21].

We apply this strategy across all three architectures, though the implementation differs due to the nature of the models:

1. **Recurrent Models (Seq2Seq & Pointer Network):** For the RNN-based architectures, Teacher Forcing is applied sequentially. During the forward pass, the decoder receives the ground-truth token y_{t-1} explicitly at each time step to compute the hidden state and output for time t [2].
2. **Transformer:** As the Transformer processes sequences in parallel, Teacher Forcing is implemented implicitly via the **Look-Ahead Mask** described previously. By masking future positions, the self-attention mechanism at position t is restricted to attending only to the ground-truth sequence indices $[0, t - 1]$, effectively replicating the Teacher Forcing behaviour without a recurrent loop [22, 5].

4.4 The Application Programming Interface (API)

The system exposes its core functionalities through a RESTful API, facilitating programmatic interaction with the implemented neural architectures. This interface serves as the primary gateway for data ingestion and inference execution.

4.4.1 Endpoints

`/run/{model_type}`

This POST endpoint provides a unified interface for sequence processing across different model architectures (**Transformer**, **Pointer Network**, or **Seq2Seq**). Once selected it returns a processed sequence made from the input data, including refitting.

`/run/{model_type}/int : n/`

This POST endpoint extends the interface to support multiple sequence generation. It accepts an integer parameter n , executing the selected model architecture n times to return a list of n alternative processed sequences.

`/check/`

This POST endpoint will count the number of **overlaps** on a given sequence, based on configuration data.

5. Experiments and Results

5.1 Task Performance

Performance is measured by how well the model can take an input with overlapping data and rearrange the tasks to minimize overloads. Although the operational constraints of the target problem typically limit sequences to batches of roughly 100 objects, the following results also evaluate the model’s scalability beyond this range.

5.1.1 Evaluation Metrics

To objectively measure the performance of the model in overlap reduction (1.7), we monitor results using a performance ratio:

$$\text{ratio} = \frac{O_{predicted}}{O_{source}} \quad (5.1)$$

where O_{source} is the total number of overlaps of the shuffled input sequence, and $O_{predicted}$ is the total number of overlaps of the predicted sequence. The closer the ratio is to 0, the better the model performs. A value above 1 indicates the model is yielding worse results than the initial shuffled state.

The Improvement rate (I) used in the tables is defined as:

$$\text{Improvement} = (1 - \frac{O_{predicted}}{O_{source}}) \times 100\% \quad (5.2)$$

The testing data is generated using a random number generator with no seed to ensure variability across test runs. The values in the following tables are based on these metrics. Note that the data has an optimal solution before shuffling where $O_{predicted} = 0$, as per the data generation algorithm in 3.1.4.

5.1.2 Pointer Network Performance

Table 5.1: Test-size of 10

Run	Ratio (R)	Improvement (I)
Run #1	14/72	80.56%
Run #2	15/68	77.94%
Run #3	21/67	68.66%
Avg		75.72%

Table 5.2: Test-size of 100

Run	Ratio (R)	Improvement (I)
Run #1	188/713	73.63%
Run #2	183/741	75.30%
Run #3	180/719	74.97%
Avg		74.63%

Table 5.3: Test-size of 1000

Run	Ratio (R)	Improvement (I)
Run #1	2008/7208	72.14%
Run #2	2013/7234	72.17%
Run #3	2031/7266	72.05%
Avg		72.12%

Table 5.4: Test-size of 10000

Run	Ratio (R)	Improvement (I)
Run #1	20329/72702	72.04%
Run #2	20001/72463	72.40%
Run #3	20151/72567	72.23%
Avg		72.22%

5.1.3 Transformer Performance

Table 5.5: Test-size of 10

Run	Ratio (R)	Improvement (I)
Run #1	7/80	91.25%
Run #2	4/58	93.10%
Run #3	8/64	87.50%
Avg		90.62%

Table 5.6: Test-size of 100

Run	Ratio (R)	Improvement (I)
Run #1	73/721	89.88%
Run #2	76/734	89.85%
Run #3	71/706	89.94%
Avg		89.89%

Table 5.7: Test-size of 1000

Run	Ratio (R)	Improvement (I)
Run #1	693/7276	90.48%
Run #2	686/7137	90.39%
Run #3	656/7268	90.97%
Avg		90.61%

Table 5.8: Test-size of 10000

Run	Ratio (R)	Improvement (I)
Run #1	5259/72219	92.72%
Run #2	5553/72584	92.36%
Run #3	5518/72422	92.38%
Avg		92.49%

5.1.4 Seq2Seq performance

Table 5.9: Test-size of 10

Run	Ratio (R)	Improvement (I)
Run #1	23/78	70.51%
Run #2	16/71	77.46%
Run #3	19/71	73.24%
Avg		73.74%

Table 5.10: Test-size of 100

Run	Ratio (R)	Improvement (I)
Run #1	200/708	71.75%
Run #2	190/760	75.00%
Run #3	203/717	71.69%
Avg		72.81%

Table 5.11: Test-size of 1000

Run	Ratio (R)	Improvement (I)
Run #1	2098/7171	70.74%
Run #2	1987/7236	72.54%
Run #3	2063/7362	71.96%
Avg		71.75%

Table 5.12: Test-size of 10000

Run	Ratio (R)	Improvement (I)
Run #1	20495/72675	71.80%
Run #2	20542/72830	71.79%
Run #3	20262/72554	72.07%
Avg		71.89%

5.2 Production Dataset

We obtained an official dataset from a production run. However, the raw data contained several inconsistencies that required resolution before it could be used for training. Hence a script for generated dummy dataset based on the original was made for simulating this task, where borrowing and tighter fits are more commonplace than actual production data. (At least from what we saw from it) In theory this would be beneficial as the model is then trained on "harder" sequences, thus sequences with more room for error and wider margins should perform better. How the data was generated is further discussed in 3.1.4.

6. Discussion

6.1 Interpretation of Results

The evaluated models demonstrated strong overall performance, with the Transformer architecture notably exceeding initial projections. The Transformer achieved an Improvement (5.1.1) of 93% at most on unseen test data, with an average of about 90%.

While this result indicates strong generalization to new sequences, the exceptionally high performance warrants scepticism regarding the nature of the synthetic dataset. Since the data is generated via a constructive "solved puzzle" algorithm (3.1.4), the resulting tasks contain inherent "fingerprints" of the generation logic. These fingerprints consist of the deterministic *Gap* and the relativistic *size* calculations, which are perfections that will not be present in real-life data.

Furthermore, even though the input sequences are freshly generated and then shuffled during testing, the relationships between compatible tasks remain encoded in their feature vectors. It is highly probable that the Transformer, utilizing its global self-attention mechanism, has successfully "reverse-engineered" these generative artifacts. Rather than learning abstract scheduling principles, the model has likely learned to identify the specific "jigsaw" edges created by the constructive algorithm. This allows it to reconstruct the original ground truth with high fidelity. The problem thus lies in overfitting, but not in the traditional sense of Input data \subset Training Data.

Adding to this, the use of Cross-Entropy Loss combined with Teacher Forcing, (which was implemented in the Transforming using a no-peek mask 4.3) may have influenced these results. While these methods are used to speed up the training process and mimic the correct order of the input data, they can cause the Transformer to become over-optimized. Thus the model may only perform well on generated data that uses the *exact same* parameters as the training set.

This hypothesis is further supported by the performance gap between the Transformer (90%) and the RNN-Based (Seq2Seq and Pointer Network) models (approximately 75%). During runtime the Transformer can inspect the entire shuffled pool of tasks simultaneously to find optimal pairings while the RNNs must attempt to reconstruct the puzzle linearly, which makes it harder to spot these global, puzzle piece connections.

6.2 Limitations

6.2.1 Testing and Training Data

Due to the limited size and inconsistency of available production data, this study relies on generated synthetic data (5.2). Although this dataset was designed to adhere to operational constraints, the absence of real-world validation, and edge-cases not accounted for within sequencing, limits our ability to confirm with full certainty that the models' performance in a live production environment will produce feasible results at all.

6.2.2 Hardware and Resource Limitations

The training process was strictly bound by the available VRAM. The Transformer architecture, which has a quadratic memory complexity relative to sequence length, frequently triggered *CUDA out of memory* errors during experimentation.

To maintain training stability, it was necessary to reduce the batch size. However, small batch sizes introduce gradient noise, making it computationally infeasible to converge effectively on a massive dataset (millions of samples). Consequently, the training dataset was capped at 500,000 samples to balance memory constraints with training duration. Future work utilizing hardware with higher VRAM capacities would allow for larger batch sizes, enabling the model to learn from the millions of examples required for optimal generalization.

6.2.3 Improvement Metrics

The binary focus on solely reducing the quantity of overlaps, without measuring their duration, is missing the forest for the trees. Although the primary objective is to minimize station overloads, a purely count-based metric fails to capture improvements in overall cycle time and station utilization. For instance, one sequence might result in 10 overlaps producing a total downtime of 400 cmin, whereas another sequence with 30 overlaps might only incur 100 cmin of total downtime.

Furthermore, it is usually not ideal to rely solely on other stations to finish in time, an additional metric for measuring "drift usage" could have been implemented as to not systematically overwork the human operators along the assembly-line.

6.3 Future Work

Future iterations of this research should prioritize bridging the gap between synthetic success and real-world application. While the current model demonstrates strong heuristic learning, scaling the training data via better computing hardware could help resolve

the remaining overloads. Specifically, optimizing the data serialization pipeline would enable the processing of millions of sequences, potentially allowing the Transformer to generalize from "strong approximation" to "perfect solution."

To mitigate the risk of the model overfitting to specific generative heuristics (6.1), future data generation pipelines should introduce stochastic variability in the "Gap" constant and centering logic. By training on datasets with irregular spacing and intentional noise, the model would be forced to learn robust general scheduling principles rather than simply reverse-engineering the constructive algorithm's fixed rules.

Additionally, it would be valuable to investigate the feasibility of Online Learning paradigms. Implementing a Human-in-the-Loop (HITL) strategy would allow the model to adapt in real-time to operator overrides. This would effectively capture the true "knowledge" of the assembly line reasoning that cannot be fully encapsulated in a synthetic training set.

Bibliography

- [1] J. L. Ba, J. R. Kiros, and G. E. Hinton, *Layer Normalization*, arXiv preprint arXiv:1607.06450, 2016.
- [2] A. Dupuis, C. Dadouchi, and B. Agard, *A decision support system for sequencing production in the manufacturing industry*, *Computers & Industrial Engineering*, vol. 185, p. 109686, 2023.
- [3] A. Bay, B. Sengupta, *Approximating meta-heuristics with homotopic recurrent neural networks*, arXiv preprint arXiv:1709.02194, 2017.
- [4] I. Pointer, *Programming PyTorch for Deep Learning*, ISBN: 9781492045359, O'Reilly Media, 2019.
- [5] A. Vaswani, N. Shazeer, N. Parmar, J. Uszkoreit, L. Jones, A. N. Gomez, Ł. Kaiser, and I. Polosukhin, *Attention is All You Need*, Advances in Neural Information Processing Systems (NeurIPS), vol. 30, 2017.
- [6] C. Fink, O. Schelén, and U. Bodin, *Work in progress: Decision support system for rescheduling blocked orders*, Department of Computer Science, Electrical and Space Engineering, Luleå University of Technology, 2023.
- [7] O. Vinyals, M. Fortunato, and N. Jaitly, *Pointer Networks*, Department of Mathematics, University of California Berkeley, 2015.
- [8] E. Stevens, L. Antiga, T. Viehmann, *Deep Learning with PyTorch*, ISBN: 9781617295263, Manning Publications, 2020.
- [9] S. Hochreiter, *The vanishing gradient problem during learning recurrent neural nets and problem solutions*, Institut für Informatik, Technische Universität München, D-80290, 1998.
- [10] L. Chen, L. Zhou, M. Zhou, X. Lu, Y. Zhu, W. Song, Z. Lu, J. Li, *Deep Reinforcement Learning Based Dynamic Scheduling of Random Arrival Tasks in Cloud Manufacturing*, Proceedings of the 6th International Conference on Universal Village (UV), 2022.

- [11] T. Mitchell, *Machine Learning*, 9780070428072, McGraw-Hill, 1997.
- [12] J. Devlin, M.-W. Chang, K. Lee, K. Toutanova, *BERT: Pre-training of Deep Bidirectional Transformers for Language Understanding*, Proceedings of NAACL-HLT, 2019.
- [13] P. Giannoulis, Y. Pantis, C. Tzamos, *Teaching Transformers to Solve Combinatorial Problems through Efficient Trial & Error*, Advances in Neural Information Processing Systems (NeurIPS), 2025.
- [14] Y. Youssef, P. R. M. de Araujo, A. Noureldin, S. Givigi, *TRATSS: Transformer-Based Task Scheduling System for Autonomous Vehicles*, arXiv preprint arXiv:2504.05407, 2025.
- [15] I. Loshchilov and F. Hutter, *Decoupled Weight Decay Regularization*, In ICLR, 2019.
- [16] D. Bahdanau, K. Cho, Y. Bengio, *Neural Machine Translation by Jointly Learning to Align and Translate*, In ICLR, 2015.
- [17] R. Pascanu, T. Mikolov, Y. Bengio, *On the difficulty of training Recurrent Neural Networks*, In ICML, 2013.
- [18] O. Vinyals, S. Bengio, M. Kudlur, *Order Matters: Sequence to Sequence for Sets*, In ICLR, 2016.
- [19] S. Hammedi, A. Namoun, M. Shili, *Reinforcement Learning for Real-Time Scheduling in Dynamic Reconfigurable Manufacturing Systems*, International Journal of Advanced Computer Science and Applications (IJACSA), 2025.
- [20] C. Zhang, M. Juraschek, C. Herrmann, *Deep reinforcement learning-based dynamic scheduling for resilient and sustainable manufacturing: A systematic review*, Journal of Manufacturing Systems, 2024.
- [21] M. Sangiorgio, F. Dercole, *Robustness of LSTM neural networks for multi-step forecasting of chaotic time series*, Chaos, Solitons & Fractals, 2020.
- [22] T. Mihaylova, A. F. T. Martins, *Scheduled Sampling for Transformers*, In ACL, 2019.